Accepted Manuscript

Flexural Properties, Thermal Conductivity and Electrical Resistivity of Prealloyed and Master Alloy Addition Powder Metallurgy Ti-6Al-4V

L. Bolzoni, E.M. Ruiz-Navas, E. Gordo
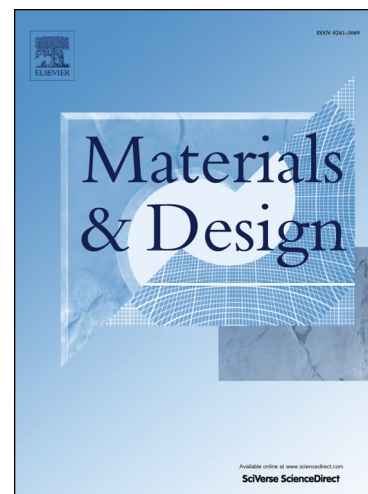
Please cite this article as: Bolzoni, L., Ruiz-Navas, E.M., Gordo, E., Flexural Properties, Thermal Conductivity and Electrical Resistivity of Prealloyed and Master Alloy Addition Powder Metallurgy Ti-6Al-4V, *Materials and Design* (2013), doi: http://dx.doi.org/10.1016/j.matdes.2013.06.036

Flexural Properties, Thermal Conductivity and Electrical Resistivity of Prealloyed and Master Alloy Addition Powder Metallurgy Ti-6Al-4V

L. Bolzoni, E.M. Ruiz-Navas, E. Gordo

Departamento de Ciencia e Ingeniería de Materiales e Ingeniería Química

Universidad Carlos III de Madrid

Avda. de la Universidad, 30, 28911 Leganés (Madrid), Spain

e-mail: bolzoni.leandro@gmail.com, lbolzoni@ing.uc3m.es, +34916249482

Abstract

A comparison between the properties achievable by processing the Ti-6Al-4V alloys by means of two powder metallurgy approaches, precisely prealloyed and master alloy addition, was carried out. Prealloyed and master alloy addition hydride-dehydirde powders characterised by an irregular morphology were shaped by means of cold uniaxial pressing and high vacuum sintered considering the effect of the variation of the sintering temperature and of the dwell time. Generally, the higher the temperature and the longer the dwell time, the higher the relative density and, consequently, the better the mechanical performances. Nevertheless, a higher processing temperature or a longer time leads also to some interstitials pick-up, especially oxygen, which affects the mechanical behaviour and, in particular, lowers the ductility. Although some residual porosity is left by the pressing and sintering route, mechanical properties, thermal conductivity and electrical resistivity values comparable to those of the wrought alloy are obtained.

Keywords: titanium alloys, powder metallurgy, flexural properties, thermal conductivity, electrical resistivity

1. Introduction

The interest for titanium as engineering material started approximately 80 years ago thanks to the special attention paid by the aeronautic industry in this material and, therefore, it is considered a relatively new engineering material with respect to other metals, such as copper or steel. The interest was dictated by the particular combination of properties that titanium can provided, precisely: the highest strength to density ratio among metals, high strength at relatively high temperatures (up to 550ºC), outstanding corrosion resistance and excellent biocompatibility [1-3]. From this, titanium and its alloys should be widely used in many different sectors and applications but, actually, they are mainly employed in high-demanding industries like the aeronautic industry, in highly corrosive environments, in racing cars and also to produce medical and dental devices and prosthesis. This is principally due to the fact that titanium is an expensive metal both to extract and process due to its affinity for interstitial elements such as oxygen, nitrogen and carbon which, even in small quantity, significantly lower the ductility [3, 4].

Among the over 3000 titanium alloys developed and tested during the extensive research carried out on the 1950's, the alpha-beta Ti-6Al-4V alloy has been the most successful, becoming the titanium workhorse, and it is still one of the most popular and employed. The success of this alloy is mainly due to its versatility in terms of properties which can be adjusted for specific applications by means of different thermomechanical processes and heat treatments. Specifically, these methods are employed to modify the relative amount and features of the microconstituents, namely the alpha and the beta phases. Even though titanium and its alloys are principally produced by means of conventional metallurgy processes such as ingot metallurgy or casting, they have also been considered for powder metallurgy (PM) techniques. This because PM techniques are processing methods that allow a reduction in production costs because approximately 90% of the raw material is used and there is the possibility to avoid or limit machining, being net-shape or near-net-shape techniques [5].

2

Concerning the PM of titanium, in general, there are two approaches as a function of the way in which the alloying elements are added [6]. In the case of prealloyed (PA) powders each powder particle has already the final composition whereas in the blended elemental (BE) approach, elemental titanium powder is mixed with alloying elements powders. In this last case it does exist also the possibility to add the alloying elements by means master alloy powders which can be specifically designed in order to adjust the final composition. Both approaches have technological advantages and disadvantages correlated with the nature of the starting powders but the master alloy addition approach has been defined has the cheapest way to obtain titanium alloys with the desired composition [7]. The great majority of the researches done on the PM of titanium focus on the Ti-6Al-4V alloy and were performed in the 1980's starting from sponge titanium powders [8]. The problem of this type of powder is the presence of residual salt, in particular chlorides, left from the Kroll reduction process which forms porosity filled with gas during sintering which prevent the complete densification of the products. This porosity filled with gas is difficult to close by means of post-processing techniques, like hot isostatic pressing, and makes the material unweldable. Lately, titanium alloys and especially the Ti-6Al-4V alloy have been considered for their production by means of advanced powder metallurgy techniques [9-15].

The aim of this work is to study the influence of the sintering parameters, namely the sintering temperature and the dwell time, on the final properties of the PM Ti-6Al-4V alloy. In particular, the study considers both prealloyed and master alloy addition powders obtained by means of the hydride-dehydride (HDH) comminution process in order to highlight possible significant difference induced by the nature of the starting powders. The employment of HDH powders avoid the problems related to the presence of the chlorides. The work considers the characterisation of relative density, chemical analysis, mechanical properties, microstructural and failure analysis as well as the correlation with the processing parameters. The study is

3

completed by the determination of the thermal conductivity and the electrical resistivity of the PM Ti-6Al-4V samples sintered under diverse combinations of temperature/time.

2. Experimental Procedure

In this study the behaviour of a hydride-dehydride (HDH) prealloyed Ti-6Al-4V powder purchased from Se-Jong Materials Co. Ltd. was compared to that of an irregular hydride-dehydride Ti-6Al-4V powder produced considering the master alloy addition approach. In particular, this last powder was obtained by mixing a HDH elemental titanium powder with an Al:V master alloys both of them supplied by GfE Gesellschaft für Elektrometallurgie mbH. The details of the development of the master alloy and of the optimisation of its features for blend it with elemental titanium can be found else where [16]. Table 1 shows some properties of the bought and produced Ti-6Al-4V powders considered, which will be identified as Ti64-PA and Ti64-MA, respectively.

As it can be seen in Table 1, the HDH powders, which were obtained by means of comminution process, are characterised by an irregular morphology and from the results of the particle size distribution the Ti64-PA powder is somewhat finer. This aspect play an important role during sintering since the densification of the material is favoured by a smaller particle size or, in turns, by a greater surface area. This is because the reduction of the surface energy is the driving force of the sintering step. The compaction pressure applied to consolidate rectangular shaped three-point bending test samples (ASTM: B528) of the Ti64-PA powder was set to 400 MPa to prevent delamination [16]. This is because the prealloyed powder is much harder and difficult to press due to the fact that the alloying elements are already dissolved inside the titanium matrix. The compaction pressure was increased to 700 MPa, a typical value used in the PM industry, for the Ti64-MA powder which is softer and leads to a significantly lower wear-out of the shaping tools. The compaction pressure dictates the level of green density obtained in the specimens and, therefore, influences the

4

densification during sintering. Green samples were sintered in a high vacuum tubular furnace with a minimum level of vacuum of 10^{-5} mbar and employing heating and cooling rates of 5ºC/min. The study of the influence of the sintering temperature, which ranges between 1250ºC and 1350ºC, was performed using two dwell time, namely 2 hours and 4 hours. The sintered samples were characterised in terms of relative density, where the nominal values of 4.43 g/cm^3 of the wrought Ti-6Al-4V alloy [3] was used for its calculation. Microstructural analysis was carried out by means of an Olympus GX71 optical microscope. For that the samples were prepared by following the classical metallographic route (SiC papers grinding and silica gel polishing) and etched with Kroll reactant to reveal the microconstituents. A Philips XL-30 SEM equipped with an EDS detector was also employed to check the distribution and homogenisation of the alloying elements, specifically for master alloy addition materials. The same machine was also used for the study of the fracture surface. Oxygen and nitrogen contents by means of the inert gas fusion method were measured using a LECO TC 500 machine. Oxygen and nitrogen contents were determined as specified in the ASTM: E1409 standard. Vickers hardness was obtained by means of a Wilson Wolpert Universal Hardness DIGI-TESTOR 930 tester performing HV30 measurements. In the case of three-point bending test samples, the transverse-rupture-strength (TRS) was measured where the tests were carried out by means of a MicroTest three-point bending test machine using the ASTM: B528 standard as guide. The thermal conductivity at room temperature (k) was calculated on the base of the relationship between the thermal conductivity (k), the diffusivity (α), the density (ρ) and the specific heat capacity at constant pressure (C_p): $k = \alpha \cdot \rho \cdot C_p$. The thermal diffusivity (α) of the samples was measured using a Netzsch LFA 447 Nanoflash machine. Finally, the electrical resistivity was determined on the base of the measurement of the electrical conductivity using the method proposed by van der Pauw [17]. Measurements of variation of the thermal conductivity with the temperature (up to 300ºC) were carried out on samples sintered at 1250ºC during 2 hours. It is well known that C_p greatly depends on the

5

temperature but this could not be taken into account during the experiments. Therefore, the variation of the C_p with the temperature was approximated with the equation available in the literature for alpha titanium [3]: $C_p = 669.0 - (0.037188 \cdot T) - (1.080 \cdot 10^7 \cdot T^{-2})$ where T is the temperature expressed in Kelvin. The calculated C_p values were used to calculate the thermal conductivity of the sintered materials. These values were compared with the values measured directly by means of the equipment and with the data of the wrought alloy.

3. Results and Discussion

3.1 Relative density

To better understand the behaviour of the alloys during sintering and the values of relative density, it is interesting to know the green density, the volume change and the densification. More in detail, green density mean values are $72.13 \pm 0.50\%$ for Ti64-PA (shaped at 400 MPa) and $85.85 \pm 0.22\%$ for Ti64-MA (shaped at 700 MPa) due to the different compacting pressure. The volume variation induced by sintering increases either with the increment of the sintering temperature or time for both Ti64-PA and Ti64-MA. Moreover, Ti64-PA specimens obtained higher shrinkage than Ti64-MA samples, with mean values of 22% and 9% respectively, due to the lower green density. The densification of the specimens increases with sintering temperature and time and, once again, the values obtained for the Ti64-PA powder (74% on average) are much greater compared to those of the Ti64-MA powder (59% on average). This is another direct consequence of the compaction pressure which results in a lower green density and in a higher densification.

The relative density results obtained from the prealloyed (Ti64-PA) and the master alloy addition (Ti64-MA) green samples sintered under diverse processing conditions are presented in Figure 1.

6

From the data of the relative density of Ti64-PA and Ti64-MA samples (Figure 1), it can be seen that the relative density increases with the sintering temperature and is always a little bit higher for longer processing time independently of the powder production route and of the compaction pressure applied to shape the powder. In general, the increment of the sintering temperature from 1250ºC to 1300ºC seems to be more effective than from 1300ºC to 1350ºC to reach higher relative density. Concerning the doubling of the dwell time from 2 hours to 4 hours, it seems that its benefit decreases with the increment of the sintering temperature. By comparing the values of the final relative density achieved in Ti64-PA and Ti64-MA specimens, it is clear that, generally, Ti64-MA samples reach higher relative density than Ti64-PA specimens but with the exception of the samples sintered at 1350°C-4h. Moreover, the difference between Ti64-PA and Ti64-MA is much more pronounced for the lowest sintering temperature considered. This behaviour is due to the lower green density of the sample produced with the Ti64-PA powder because they were pressed at lower pressure. Nonetheless, the difference in terms of relative density between Ti64-PA and Ti64-MA decreases with the increment of the temperature due to the aspect: (1) Ti64-PA is favoured by the slightly lower particle size and (2) in the case of Ti64-MA samples part of the thermal energy supplied is spent for the diffusion and homogenisation of the alloying elements throughout the titanium matrix. Apart from Ti64-PA sintered at 1250°C either 2 hours or 4 hours, relative density values for the Ti-6Al-4V alloy ranges between 95% and 96%, similar to that obtained by other authors using elemental titanium sponge powders blended with elemental powders [18-21] or master alloys [20, 22, 23].

3.2 Microstructural analysis

Microstructural analysis was carried out to study the development of the microstructure and the evolution of the porosity and the representative micrographs of both materials are displayed in Figure 2.

7

The results of the microstructure analysis shown in Figure 2 indicate that the microconstituents of the Ti-6Al-4V titanium alloy are alpha grains and α + β lamellae typical of slow cooling α + β titanium alloy from above the beta field. For both Ti64-PA and Ti64-MA samples, it can be noticed that the size of the alpha grain becomes bigger with both the increment of the sintering time and of the processing time whereas the α + β lamellae become thinner and longer. When comparing the powder production route, the microstructure components of the Ti64-PA samples are, normally, smaller than those of the Ti64-MA specimens. The reason for the finer microstructure of Ti64-PA is the combination of smaller particle size of the starting powder and the greater thermal energy invested for the densification. From Figure 2, the microstructure of Ti64-MA is fully homogeneous as it was checked by means of SEM and EDS analysis. From the results shown in Figure 2, it can also be seen that, with the relative density values obtained, the porosity is mainly spherical, isolated and the total amount decreases with the increment of the sintering temperature and with the doubling of the processing time from 2 hours to 4 hours.

3.3 Chemical analysis

The results of the chemical analysis done on sintered samples and the values of the starting Ti64-PA and Ti64-MA powders are presented in Table 2.

The percentage of oxygen (Table 2) found in the sintered specimens of Ti64-PA stays almost constant at 0.60 wt.% for 1250ºC and 1300ºC independently of the dwell time and it increases significantly to 0.75 wt.% or 0.83 wt.% at 1350°C for 2 hours or 4 hours of sintering time, respectively. On the other hand, the oxygen content of the Ti64-MA always increases with the sintering temperature with the exception of 1300°C-2h, which is equals to 1250ºC-2h, but reaching lower values compared to Ti64-PA, especially when the samples are sintered for 4 hours. Resuming, there is always, at least, a 0.20 wt.% and a 0.12 wt.% oxygen pick-up for Ti64-PA and Ti64-MA, respectively, with respect to the content of the starting

8

powders. This contamination could derive from the handling of the powder, the air trapped in the green specimens or the different surface area of the powders. Concerning nitrogen content, as it can be noted in Table 2, there is no that big variation of this interstitial element either with the temperature or the processing time becuase the values obtained are similar and around 0.02 wt.%. Even if there has been some nitrogen pick-up with respect to the initial content of the powder, the final quantity of this element is well below the limit indicated by the international standards (0.05 wt.%) [3].

3.4 Vickers Hardness

The results of hardness measurements, represented as mean values plus standard deviation, for Ti64-PA and Ti64-MA are shown in Figure 3.

As it can be seen in Figure 3, the hardness of PM Ti-6Al-4V increases with the sintering temperature and with the processing time, reaching the maximum values at the higher temperature and for longer time. In particular, in the case of the Ti64-PA alloy the increment of the sintering temperature seems to be more beneficial than the doubling of the processing time from 2 hours to 4 hours in order to reach higher hardness. Conversely, in the case of the Ti64-MA samples, the increment of the dwell time is somewhat more effective than the increasing of the temperature. Nevertheless, the trends of the increment of the hardness shown in Figure 3 are also greatly affected by the relative amount of interstitial elements dissolved by each sample. As it could have been expected on the base of the relative density data (Figure 1), Ti64-MA samples reach higher values with respect to Ti64-PA specimens due to the lower amount of residual porosity present in the microstructure. However, the difference is not that marked because it is approximately 10 HV30 and it is due to the fact that the hardness of the Ti64-PA samples is increased significantly by the greater amount of interstitials dissolved. Similar Vickers hardness values are obtained when processing the Ti-6Al-4V alloy by means of selective laser sintering [24]. In comparison to the wrought Ti-6Al-

9

4V alloy in the annealed state, whose hardness is 321 HV [3], both Ti64-PA and Ti64-MA are rather harder, with the exception of the Ti64-PA sintered at 1250°C during 2 hours, even though of the presence of approximately 5% to 6% of residual porosity. This is justified by the higher oxygen content of the Ti64-PA and Ti64-MA samples with respect to the limit specified for the wrought alloy. In the case of the Ti64-PA specimens sintered at 1250ºC-2h, their hardness results to be lower than the wrought material because of the low relative density (92.5%).

3.5 Flexural properties

Representative examples of the bending behaviour found for the PM Ti-6Al-4V alloy submitted to bending tests are presented as load-deflection curves in Figure 4. Specifically, the curves plotted allow to compare the effect of a higher sintering temperature (1250ºC vs. 1350ºC) but constant time or a longer processing time (2h vs. 4h) for the same temperature. As it can be seen in Figure 4, Ti64-PA and Ti64-MA three-point bending samples behave similarly independently of the sintering condition even though the maximum load and deflection values change from one case to the other due to the variation of the relative density, microstructural features and amount of interstitials dissolved. In particular, the load-deflection curves shown in Figure 4 indicate that the material shows predominantly an elastic behaviour with a very little plastic deformation before fracture. Moreover, it can be stated that the flexural modulus of the sintered samples is similar since the specimens show comparable behaviour in the part of the load-deflection curve which represent the elastic behaviour of the material. The absolute value of the flexural modulus determined on PM Ti-6Al-4V specimens is not indicated because it is not an intrinsic property of the material since greatly depends on the ratio between the span length (L) of the testing configuration and the diameter of the specimen (D) as available in the literature where the increment of the L/D ratio leads to an increase of the flexural modulus [25, 26]. By means of the formula reported in the ASTM:

10

B528 standard, which is applicable to relatively brittle materials, the values of TRS were calculated and they are reported in Figure 5.

As it can be seen from the data of strength shown in Figure 5, the TRS of the Ti64-PA samples decreases with the increment of the sintering temperature. The only exception to this trend is the value of the samples sintered at 1250ºC during 2 hours which is the lowest. This is most probably due to the low relative density that characterise the samples processed with these sintering parameters. When considering the effect of the doubling of the dwell time at temperature from 2 hours to 4 hours, it can be seen that the specimens sintered during 4 hours present lower strength than their counterpart. This behaviour is primary due to the microstructural changes induced by a longer processing time (i.e. grain growth and pore coarsening) but it is also affect by the interstitial pick-up where the higher their amount the lower the strength. The same trend of the variation of TRS with the sintering temperature and processing time described for the Ti64-PA samples is useful to describe the behaviour of the Ti64-MA specimens. Nonetheless, it should be noticed that, in the case of the Ti64-MA alloy the samples sintered during 4 hours are characterised by higher TRS values in comparison to those sintered during 2 hours. This behaviour is favoured by the slightly higher relative density of the samples sintered during 4 hours but it is principally a consequence of the lower oxygen content of these specimens (see Table 2). When comparing the values of TRS obtained for each of the powder production route (prealloyed versus master alloy addition), it can be seen that Ti64-MA samples always reaches higher strength with respect to the Ti64-PA specimens. This difference in mainly due to the different level of interstitial elements dissolved by the materials in each sintering condition as it can be checked by combining the data shown in Table 2 and those of Figure 5. The TRS shown in Figure 5 is, on average, similar to the values found in the literature for wrought biomedical devices (903-1090 MPa) [27].

11

The results of the flexural strain at fracture (ε_f) as a function of the sintering condition studied are displayed in Figure 6.

From Figure 6, it can be seen that the flexural strain at fracture of Ti64-PA samples decreases with the increment of the processing temperature for both the processing times considered. This decreasing trend is due to the increment of the interstitials content dissolved by the alloy which increases with the increment of the processing temperature. From the data of the flexural strain at fracture of the Ti64-PA samples it can also be noticed that, generally, the doubling of the dwell time from 2 hours to 4 hours leads to a higher strain. The only exception to this trend are the samples sintered at 1350ºC-4h which are characterised by lowest value of flexural strain due to significantly higher oxygen content that these samples have. In the case of the Ti64-MA samples, once again the flexural strain decreases with the increment of the sintering time indicating that, as for the Ti64-PA samples, the benefit of the reduction of the residual porosity is overcome by the increment of the amount of interstitials dissolved. When comparing the flexural strain data as a function of the powder production method, it can be seen that Ti64-MA samples are always characterised by a higher strain in comparison to Ti64-PA specimens independently of the processing parameters employed to sinter the materials. The higher toughness of the Ti64-MA samples is due to the balanced effect of slightly higher relative density, lower oxygen content and coarser microstructural features with respect to the Ti64-PA specimens.

The fractographic analysis of the tensile test specimens by SEM was carried out and the results are presented in Figure 7. Due to the fact that no significant differences were found on the bases of the sintering temperature, only the micrograph corresponding the samples sintered at 1300ºC during 2 hours are shown.

From the analysis of the fracture surface (Figure 7), it can be seen that the materials fail due to transcrystalline fracture, the typical cleavage fracture mode of metals with an H.C.P. lattice, where river marking can be clearly distinguished within the grains that form the

12

microstructure [28]. This brittle fracture mode could have been expected on the base of the load-deflection curves shown in Figure 4 and it is in agreement with the results of the microstructural analysis where it was shown that the pore structure is composed of spherical and isolated pores.

3.6 Thermal conductivity and electrical resistivity

Thermal conductivity and electrical resistivity values measured on specimens sintered under different temperature/time conditions are reported in Table 2.

From the data shown in Table 2 it seems that for the Ti64-PA alloy there is no correlation between the thermal conductivity at room temperature and the relative density (Figure 1), which should be the most affecting factor. However, it seems that the increment of the relative density from 92% (1250ºC-2h) to values higher than 94% (1250ºC-4h) induces an increment of k most probably because with a 94% of relative density the pore structure is constituted by isolated pores whereas in the range of 86-94% there are still interconnected pores [5]. Conversely to Ti64-PA, the Ti64-MA alloy is characterised by the increment of the thermal conductivity at room temperature with the decreasing of the residual porosity. Moreover, it seems that a longer processing time, which induced some grain growth, leads to a smoother increment of the thermal conductivity. No significant differences were found between the values of the two types of powders since with a relative density of 95%, a k of approximately 7 W/m·ºC is obtained in both materials. Analysing the data shown in Table 2, it can be noticed that the thermal conductivity measured on pressing and sintering specimens is always higher than the nominal value of wrought Ti-6Al-4V, independently of the sintering conditions employed. It is remarkable that the highest values obtained for P&S components are similar to that of Ti-6Al-4V ELI, where the content of the interstitials is kept very low (O = 0.13 wt.% and N = 0.03 wt.%). On the other side, the electrical resistivity data for the Ti64-PA alloy (Table 2) indicate that this property increases with the relative density, which is not

13

expected but could be due to the characteristics of the residual porosity, namely the mean size and the shape, because a more uniform distribution of small pores could hinder more the movement of the electrons than a lower amount of pores of bigger size. The electrical resistivity measured in Ti64-MA alloy specimens has two opposite trends depending on the sintering time: it slightly decreases for 2 hours of dwell time and it increases a little for 4 hours. Nonetheless, the variation of the electrical resistivity is quite limited and it is most probably due to the counterbalancing effect of: (1) presence of residual porosity probably filled with gas, (2) microstructural features (relative amount of alpha and beta phases as well as grain boundaries) and (3) amount of interstitials dissolved which act as lattice defect. Comparing the data of electrical resistivity of Ti64-PA and Ti64-MA, the former are slightly higher mainly due to the higher equivalent oxygen content. Finally, the electrical resistivity of Ti64-PA and Ti64-MA is, generally, higher that that of the wrought alloy (Table 2) due to the amount of interstitials and the presence of the residual porosity.

The variation of the thermal conductivity with the temperature, which was measured on the Ti64-PA and Ti64-MA samples sintered at 1250ºC during 2 hours, is presented in Figure 8. As it can be seen in Figure 8, the thermal conductivity of pressing and sintering Ti-6Al-4V components increases with the temperature independently of the PM approach used to obtain the alloy. This increment is mainly due to the thermal energy supplied to the system, which results in a higher mobility (longer mean free path) of electrons and phonons through the material in this range of temperature. Nonetheless, it can also be seen that Ti64-MA samples are characterised by higher thermal conductivity, in agreement with the thermal conductivity at room temperature data shown in Table 2, due to the lower percentage of residual porosity present in the microstructure. From the data shown in Figure 8, it can also be seen that this difference is kept when taking into account the effect of the temperature on the C_p value and, as expected, the values calculated are higher than those measured directly on the samples. When compared to the data available in the literature for the wrought alloy [3], powder

metallurgy Ti-6Al-4V specimens have a lower thermal conductivity starting from approximately 150ºC. More in detail, it can be seen that the thermal conductivity of the wrought alloy increases with the temperature much faster than in Ti64-PA and Ti64-MA components most probably due to the effect of the presence of the residual porosity, the microconstituents features (i.e. relative amount of H.C.P. alpha and B.C.C. beta phase) and the amount of interstitials dissolved which act as lattice defects.

4. Conclusions

From the study performed it can be concluded that:

- The employment of HDH powders permits to obtain relative density values typical for the conventional PM route without the inconvenient of the presence of the chlorides;

- The master alloy addition approach permits to obtain materials with similar properties to those of more expensive prealloyed powders;

- With the processing parameters studied, homogeneous microstructures are obtained indicating a complete diffusion of the alloying elements added as master alloy;

- Mechanical properties such as flexural strength and hardness similar to those of the wrought alloy are usually obtained with PM material;

- With the appropriate combination of sintering temperature and dwell time, comparable thermal conductivity and electrical resistivity with the wrought material can be reached.

References

[1] Lütjering G, Williams JC. Titanium: Engineering Materials and Processes. 1st ed. Manchester, UK: Springer; 2003.

[2] Leyens C, Peters M. Titanium and Titanium Alloys. Fundamentals and Applications. Köln, Germany: Wiley-VCH; 2003.

[3] Boyer R, Welsch G, Collings EW. Materials Properties Handbook: Titanium Alloys. In: International A, editor. 2nd ed. Ohio, USA; 1998.

[4] Donachie MJ. Titanium. A Technical Guide. 2nd Edition ed. Ohio, USA: ASM International; 2000.

[5] Zak Fang Z. Sintering of Advanced Materials: Fundamental and Processes. Cambridge, UK: Woodhead Publishing Limited; 2010.

[6] Froes FH. The Manufacturing of Titanium P/M. The Symposium on High Performance P/M Components. Coimbra, Portugal. 2002. p. 1-16.

[7] Hurless BE, Froes FH. Lowering the Cost of Titanium. The AMPTIAC Quarterly. 2002;6:3-10.

[8] Froes FH, Eylon D. Powder Metallurgy of Titanium Alloys. Titanium: Science and Technology. Munich - Germany. 1985. p. 267-86.

[9] Das S, Wohlert M, Beaman JJ, Bourell DL. Processing of Titanium Net Shapes by SLS/HIP. Materials & Design. 1999;20:115-21.

[10] Wu X, Liang J, Mei J, Mitchell C, Goodwin PS, Voice W. Microstructures of Laser-deposited Ti-6Al-4V. Materials & Design. 2004;25:137-44.

[11] Baufeld B, van der Biest O, Gault R. Additive Manufacturing of Ti-6Al-4V Components by Shaped Metal Deposition: Microstructure and Mechanical Properties. Materials & Design. 2010;31, Supplement 1:S106-S11.

[12] Bertol LS, Júnior WK, da Silva FP, Aumund-Kopp C. Medical Design: Direct Metal Laser Sintering of Ti-6Al-4V. Materials & Design. 2010;31:3982-8.

[13] Bolzoni L, Montealegre Meléndez I, Ruiz-Navas EM, Gordo E. Microstructural Evolution and Mechanical Properties of the Ti-6Al-4V Alloy Produced by Vacuum Hot-pressing. Materials Science and Engineering A. 2012;546:189-97.

[14] Bolzoni L, Ruiz-Navas EM, Neubauer E, Gordo E. Inductive Hot-pressing of Titanium and Titanium Alloy Powders. Materials Chemistry and Physics. 2012;131:672-9.

[15] Khan DF, Yin H, Li H, Qu X, Khan M, Ali S, et al. Compaction of Ti-6Al-4V Powder using High Velocity Compaction Technique. Materials & Design. 2013;50:479-83.

[16] Bolzoni L, Esteban PG, Ruiz-Navas EM, Gordo E. Influence of Powder Characteristics on Sintering Behaviour and Properties of PM Ti Alloys Produced from Prealloyed Powder and Master Alloy. Powder Metallurgy. 2011;54:543-50.

[17] van der Pauw LJ. A Method of Measuring Specific Resistivity and Hall Effect on Lamellae of Arbitrary Shape. Philips Technical Review. 1958;20:220-4.

[18] Ivasishin OM, Anokhin VM, Demidik AN, Savvakin DG. Cost-effective Blended Elemental Powder Metallurgy of Titanium Alloys for Transportation Application. Key Engineering Materials. 2000;188:55-62.

[19] Ivasishin OM, Savvakin DG, Moxson VS, Bondareva KA, Froes FH. High Integrity, Low Cost Titanium Powder Metallurgy Components. High-performance Metallic Materials for Cost Sensitive Applications, Proceedings. 2002:117-28.

[20] Ivasishin OM. Cost-effective Manufacturing of Titanium Parts with Powder Metallurgy Approach. Materials Forum. 2005;29:1-8.

[21] Henriques VAR, de Campos PP, Alves Cairo CA, Bressiani JC. Production of Titanium Alloys for Advanced Aerospace Systems by Powder Metallurgy. Materials Research. 2005;8:443-6.

[22] Godfrey TMT, Wisbey A, Goodwin PS, Bagnall K, Ward-Close CM. Microstructure and Tensile Properties of Mechanically Alloyed Ti-6Al-4V with Boron Additions. Materials Science and Engineering A. 2000;282:240-50.

[23] Moxson VS, Qazi JI, Patankar SN, Senkov ON, Froes FH. Low-cost CP-titanium and Ti-6Al-4V Alloys. Advanced Materials Forum I. 2002;230-2:339-43.

[24] Song B, Dong S, Zhang B, Liao H, Coddet C. Effects of Processing Parameters on Microstructure and Mechanical Property of Selective Laser Melted Ti-6Al-4V. Materials & Design. 2012;35:120-5.

[25] Alander P, Lassila LVJ, Vallittu PK. The Span Length and Cross-sectional Design Affect Values of Strength. Dental Materials. 2005;21:347-53.

[26] Stewardson DA, Shortall AC, Marquis PM, Lumley PJ. The Flexural Properties of Endodontic Post Materials. Dental Materials. 2010;26:730-6.

[27] Henry D. Materials and Coatings for Medical Devices: Cardiovascular. Ohio, USA: ASM International; 2009.

[28] Bolzoni L, Esteban PG, Ruiz-Navas EM, Gordo E. Mechanical Behaviour of Pressed and Sintered Titanium Alloys Obtained from Prealloyed and Blended Elemental Powders. Journal of the Mechanical Behavior of Biomedical Materials. 2012;14:29-38.

Figure 1. Variation of the relative density as a function of the sintering temperature for Ti64-PA (left) and Ti64-MA (right) samples.

Figure 2. Representative micrograph of samples sintered at 1250ºC-2h: a) Ti64-PA and b) Ti64-MA, at 1250ºC-4h: c) Ti64-PA and d) Ti64-MA and at 1350ºC-4h: e) Ti64-PA and f) Ti64-MA.

Figure 3. Variation of the hardness as a function of the sintering temperature for Ti64-PA (left) and Ti64-MA (right) sintered samples.

Figure 4. Representative load-deflection curves of sintered samples: a) Ti64-PA and b) Ti64-MA.

Figure 5. Variation of the transverse rupture strength (TRS) as a function of the sintering temperature for Ti64-PA (left) and Ti64-MA (right) sintered samples.

Figure 6. Variation of the flexural strain at fracture as a function of the sintering temperature for Ti64-PA (left) and Ti64-MA (right) sintered samples.

Figure 7. Fracture surface of Ti-6Al-4V tensile samples sintered at 13050ºC during 2 hours: a) Ti64-PA and b) Ti64-MA.

Figure 8 - Thermal conductivity as a function of temperature for Ti64-PA and Ti64-MA specimens.
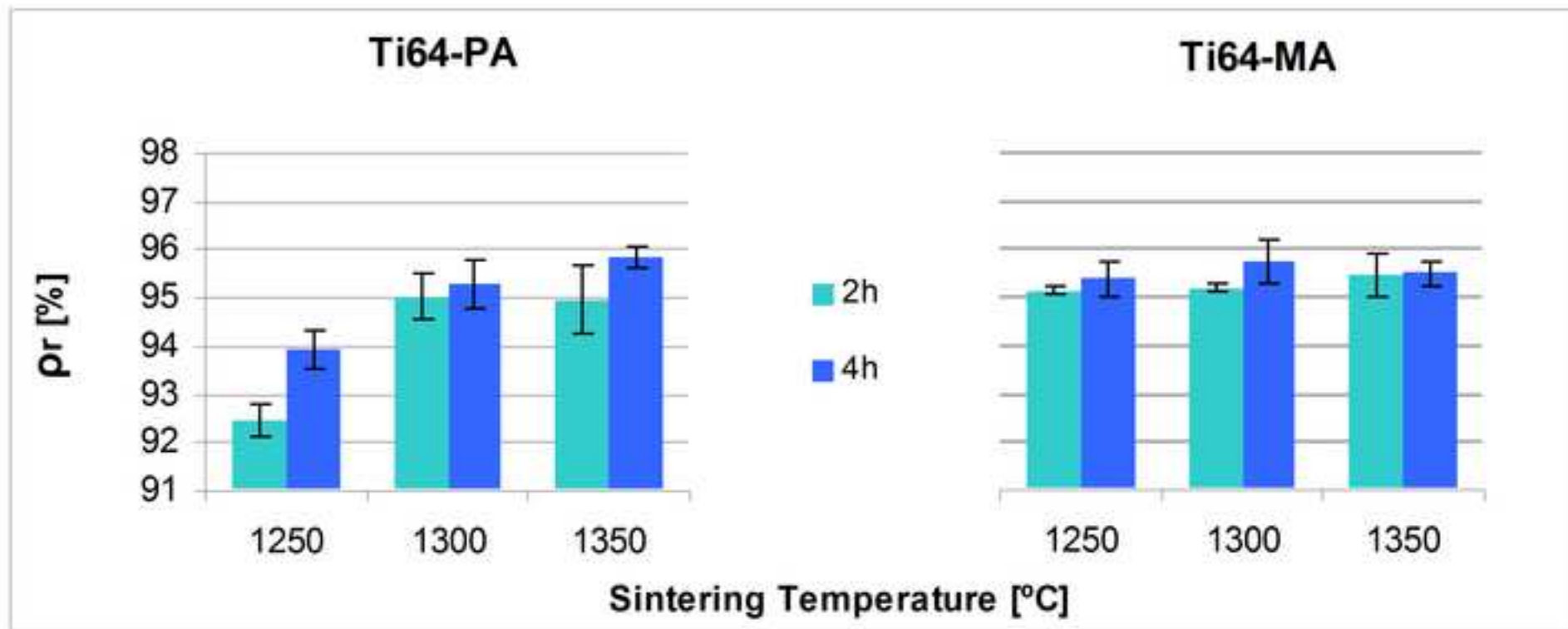
Ti64-PA   Ti64-MA

Figure 2 a)

200 μm

Figure 2 b)

200 µm

Figure 2 c)

200 μm

Figure 2 d)

200 µm

Figure 2 e)

200 µm

Figure 2 f)

200 μm

Figure 3 (colours)

Figure 4 a) (colours)

Three-point Bending Test

1250°C-4h

1250°C-2h

1350°C-4h

Load [N]

Deflection [mm]

Figure 4 b) (colours)

Three-point Bending Test

Figure 5 (colours)

Figure 6 (colours)

Figure 7 a)

Acc.V Spot Magn   Det WD |———————————————| 50 µm
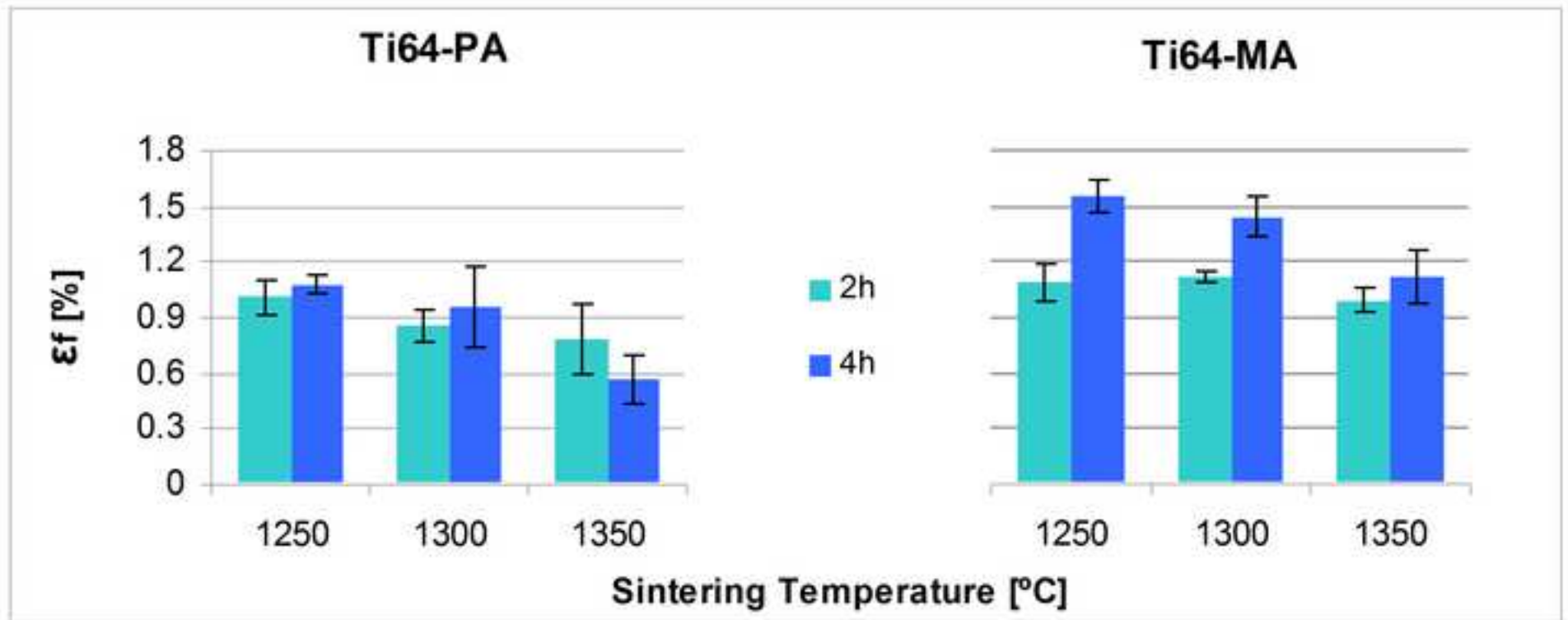20.0 kV 6.0   1000x   SE   10.3 Ti-6Al-4V_PA

Figure 7 b)

Figure 8 (colours)
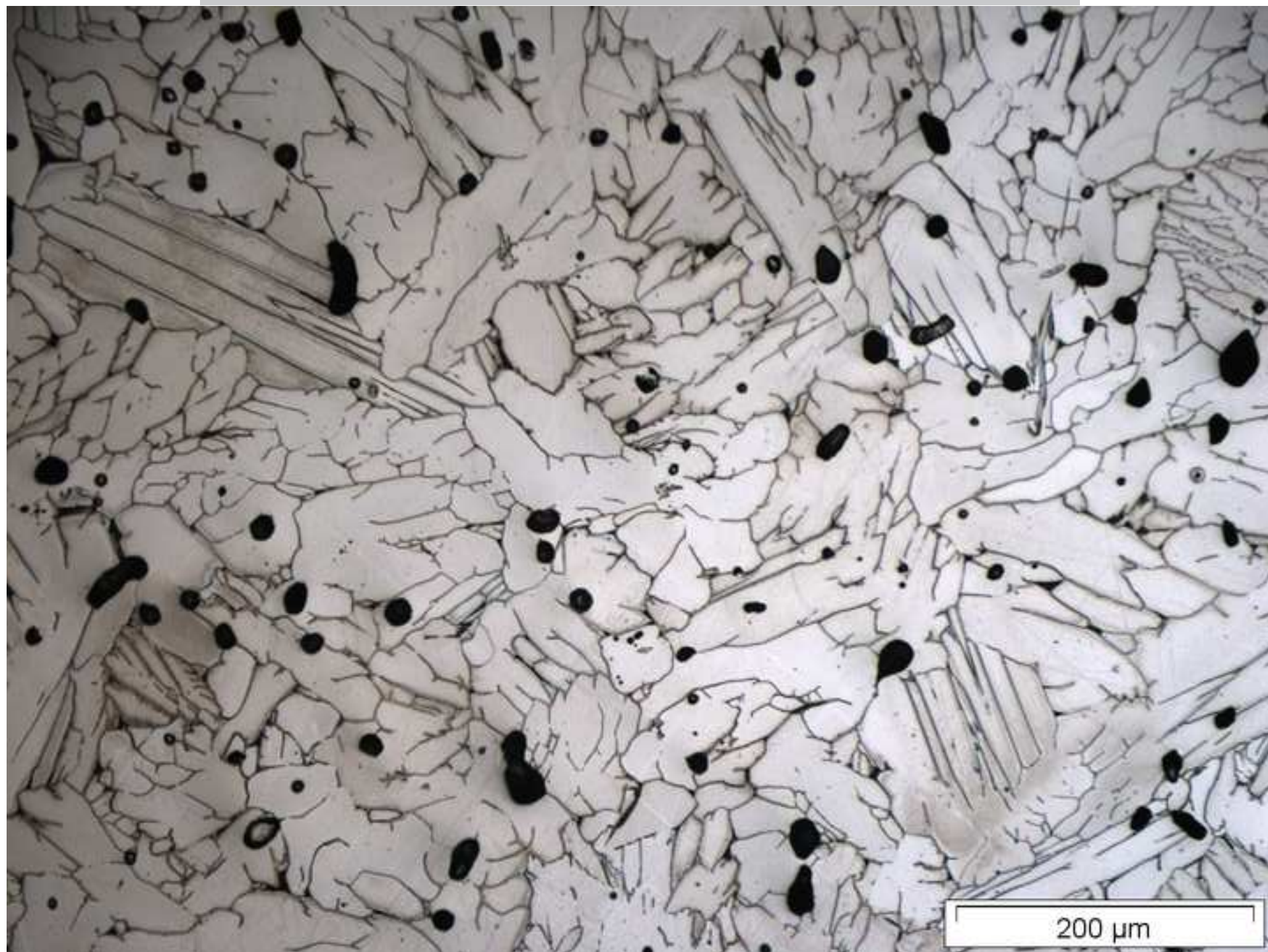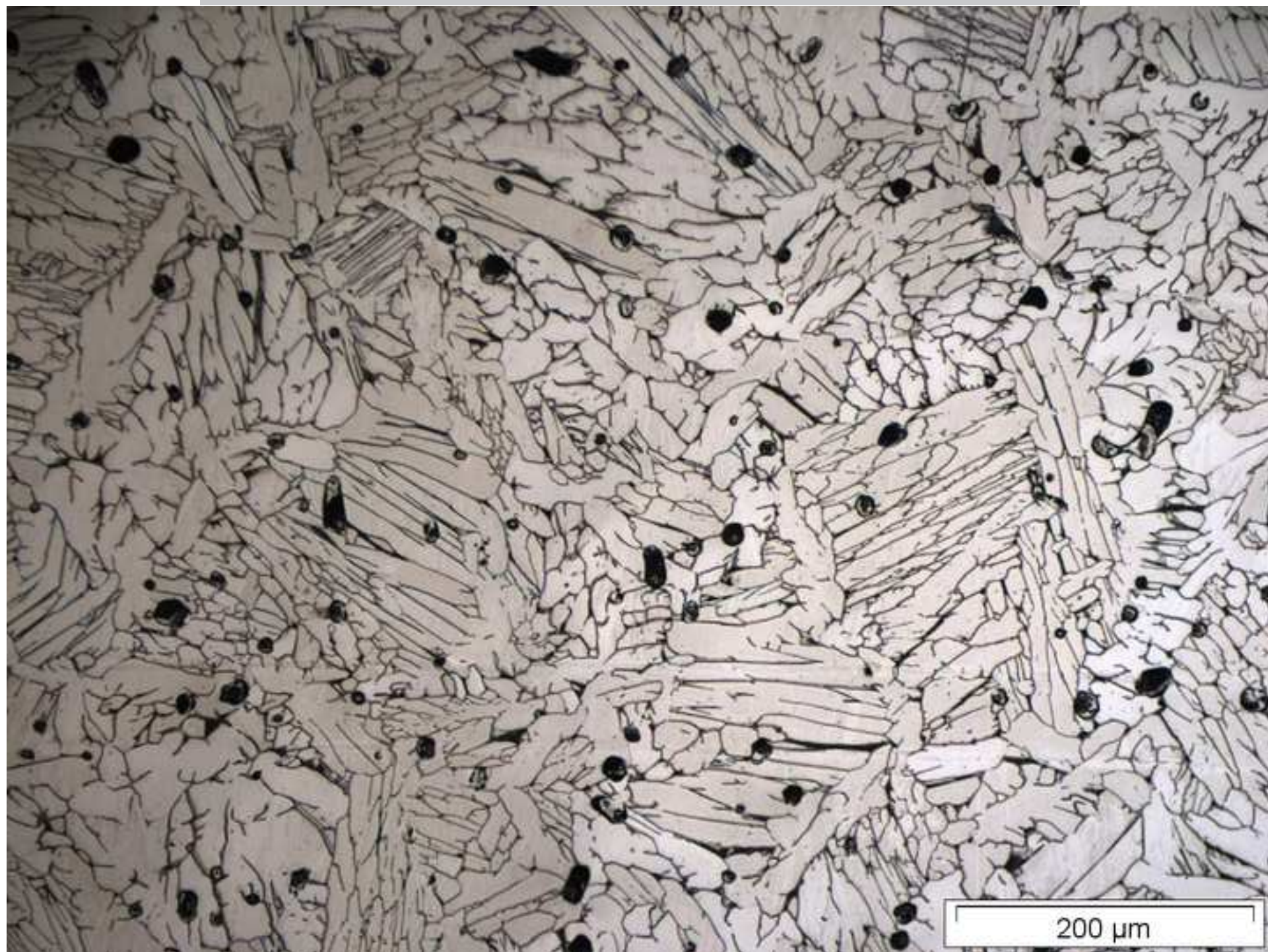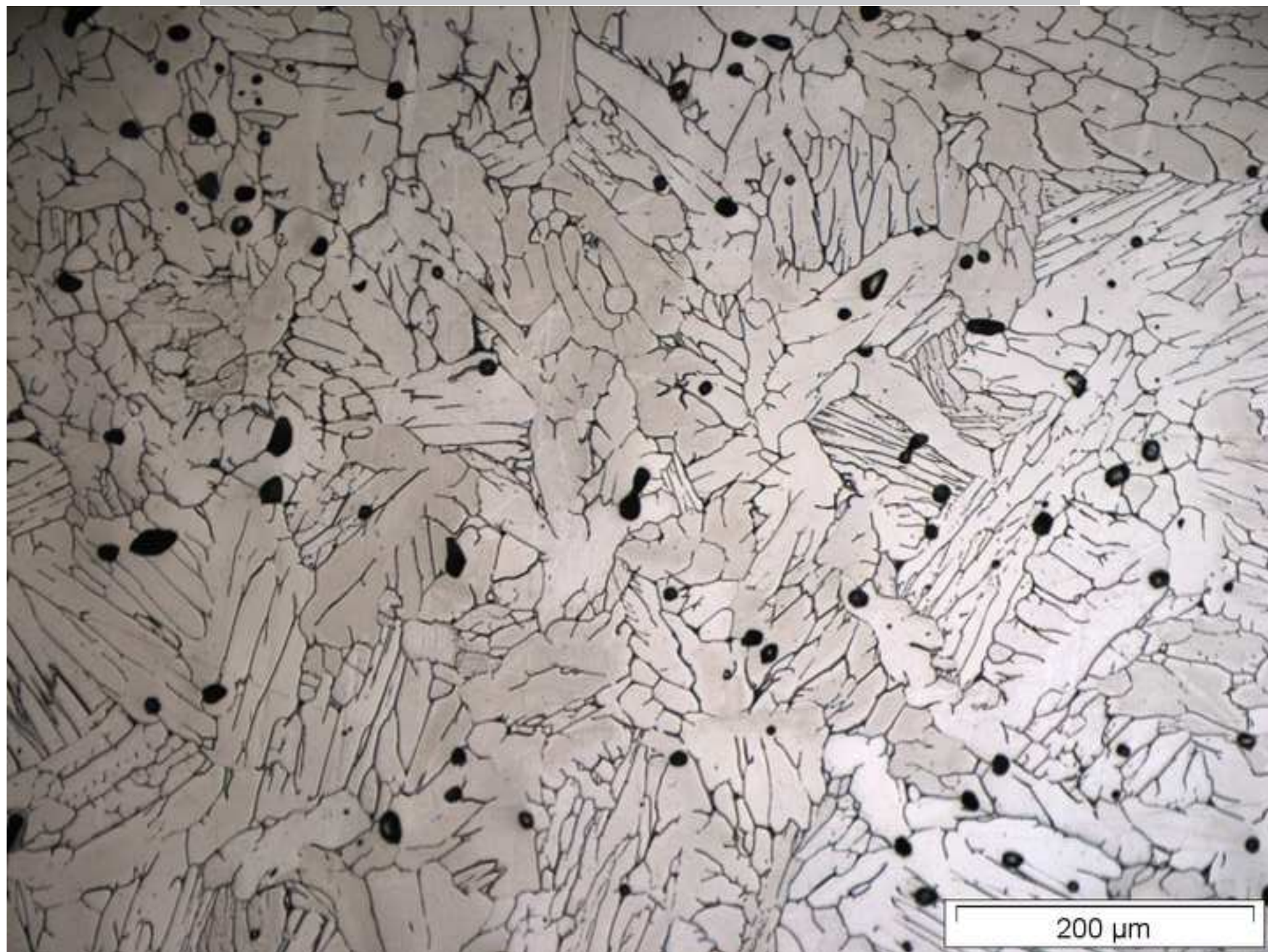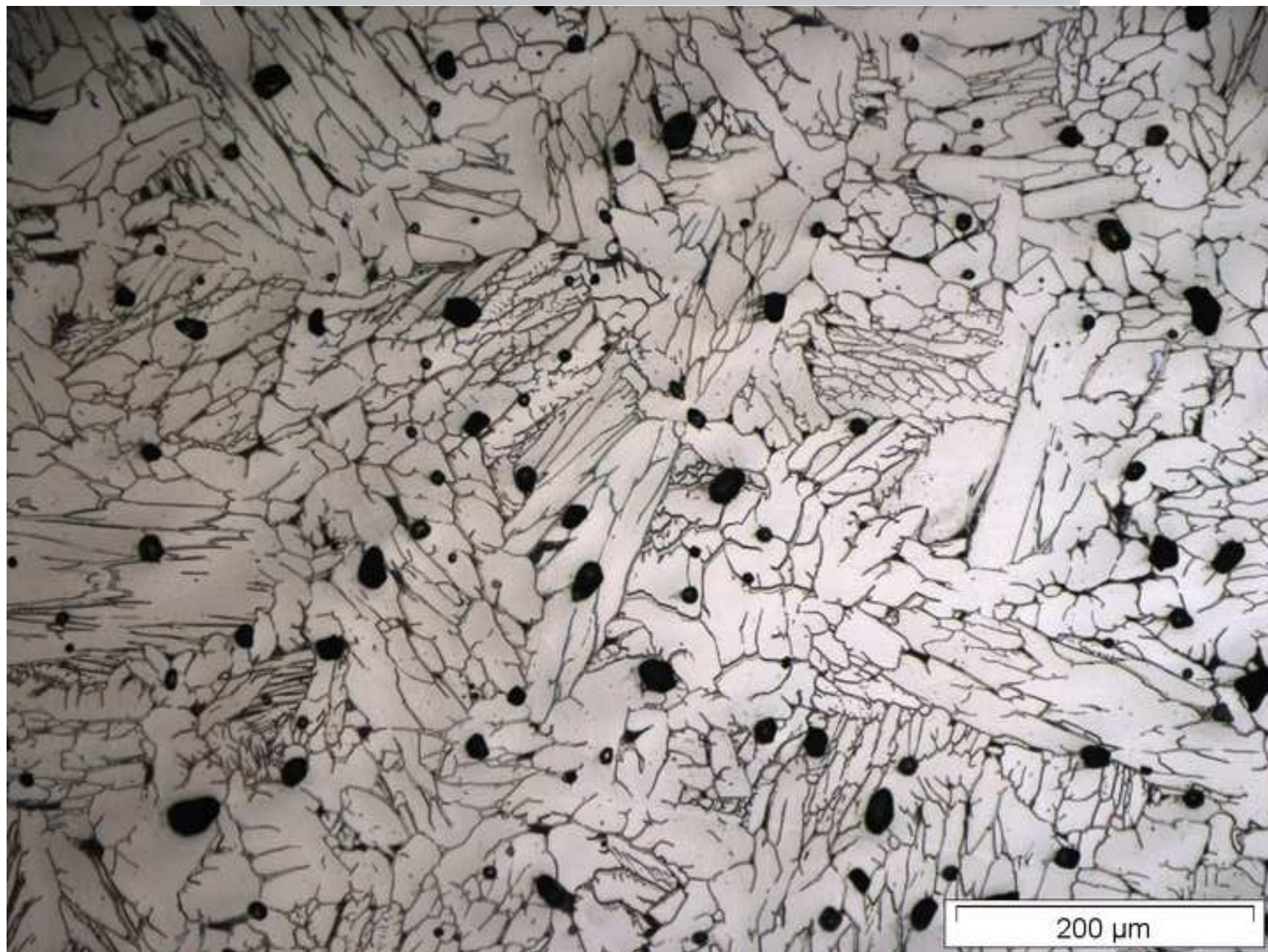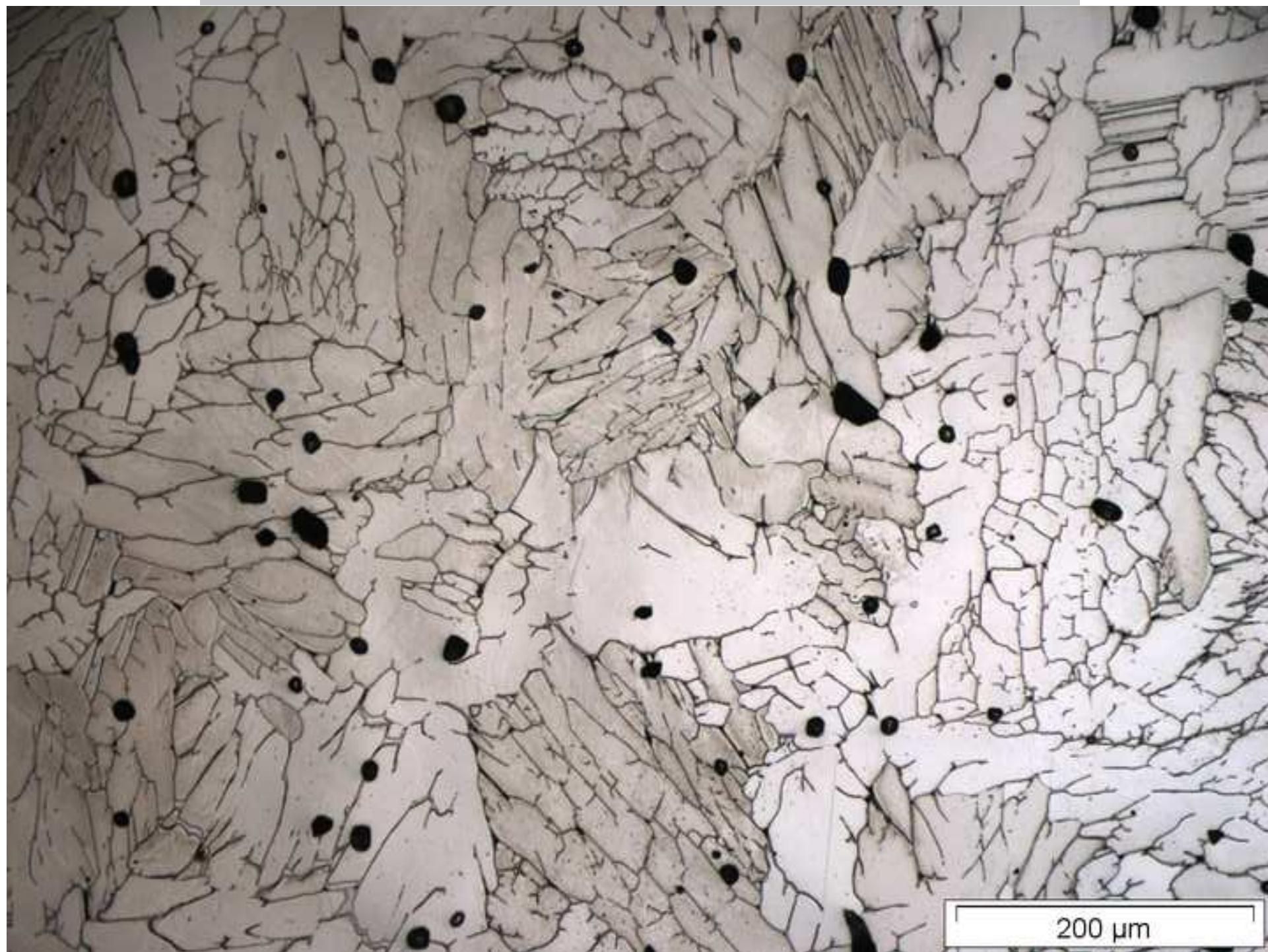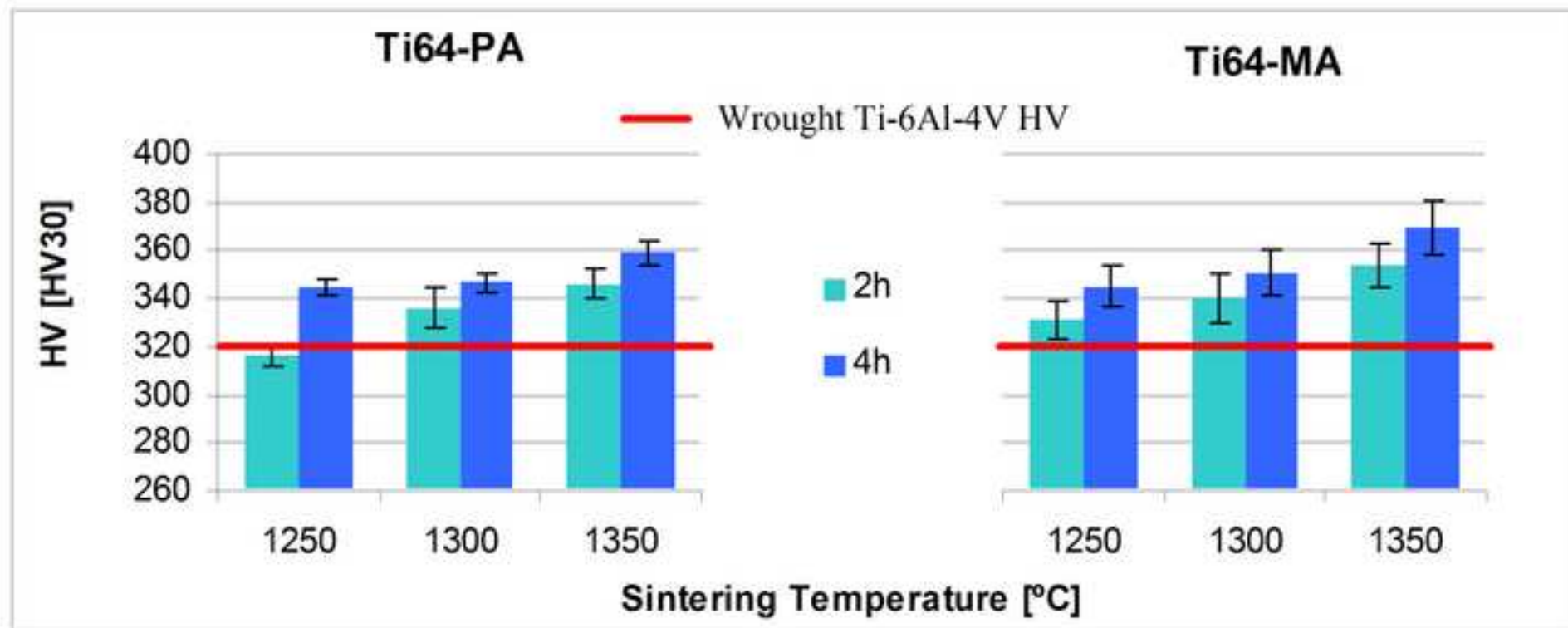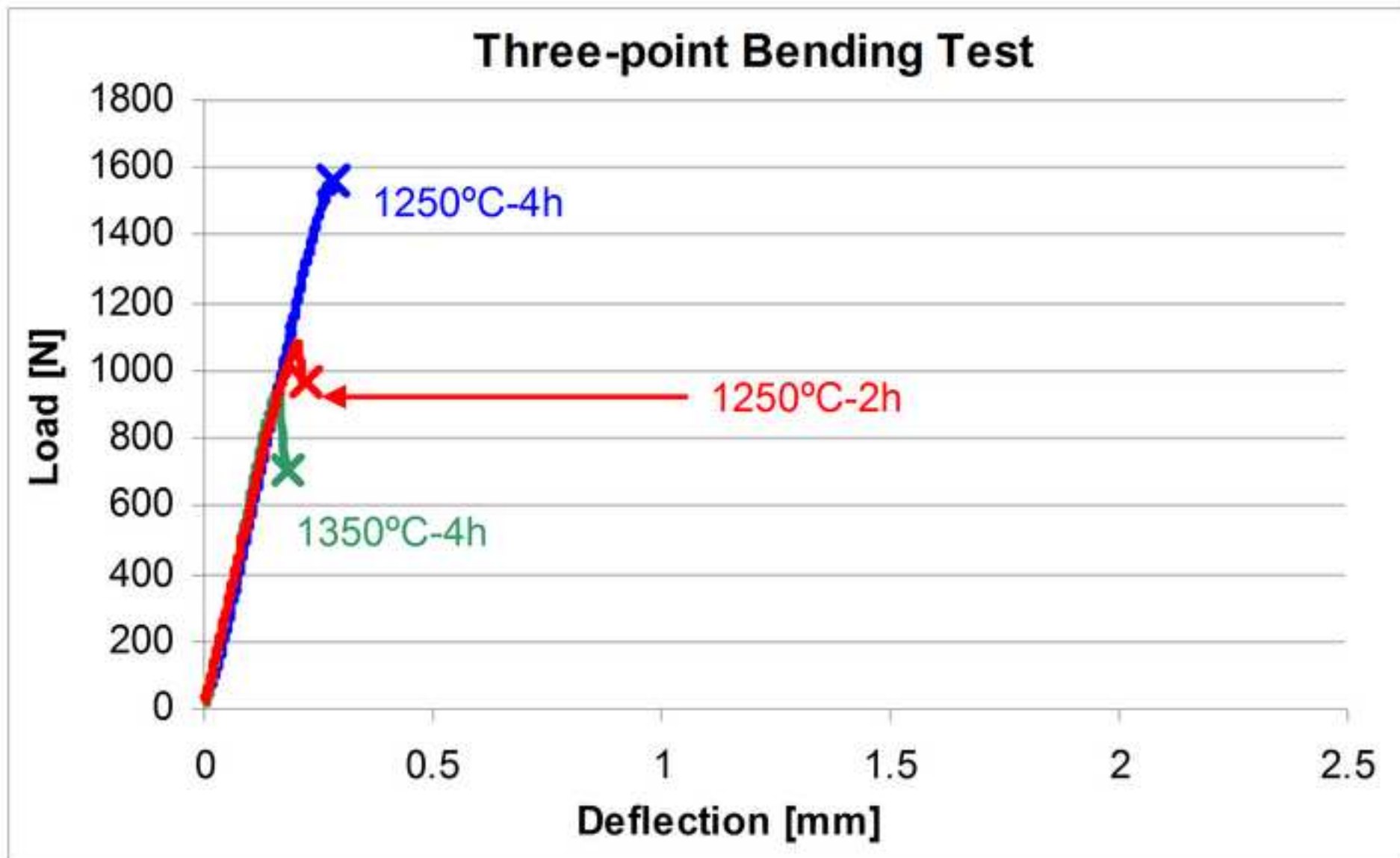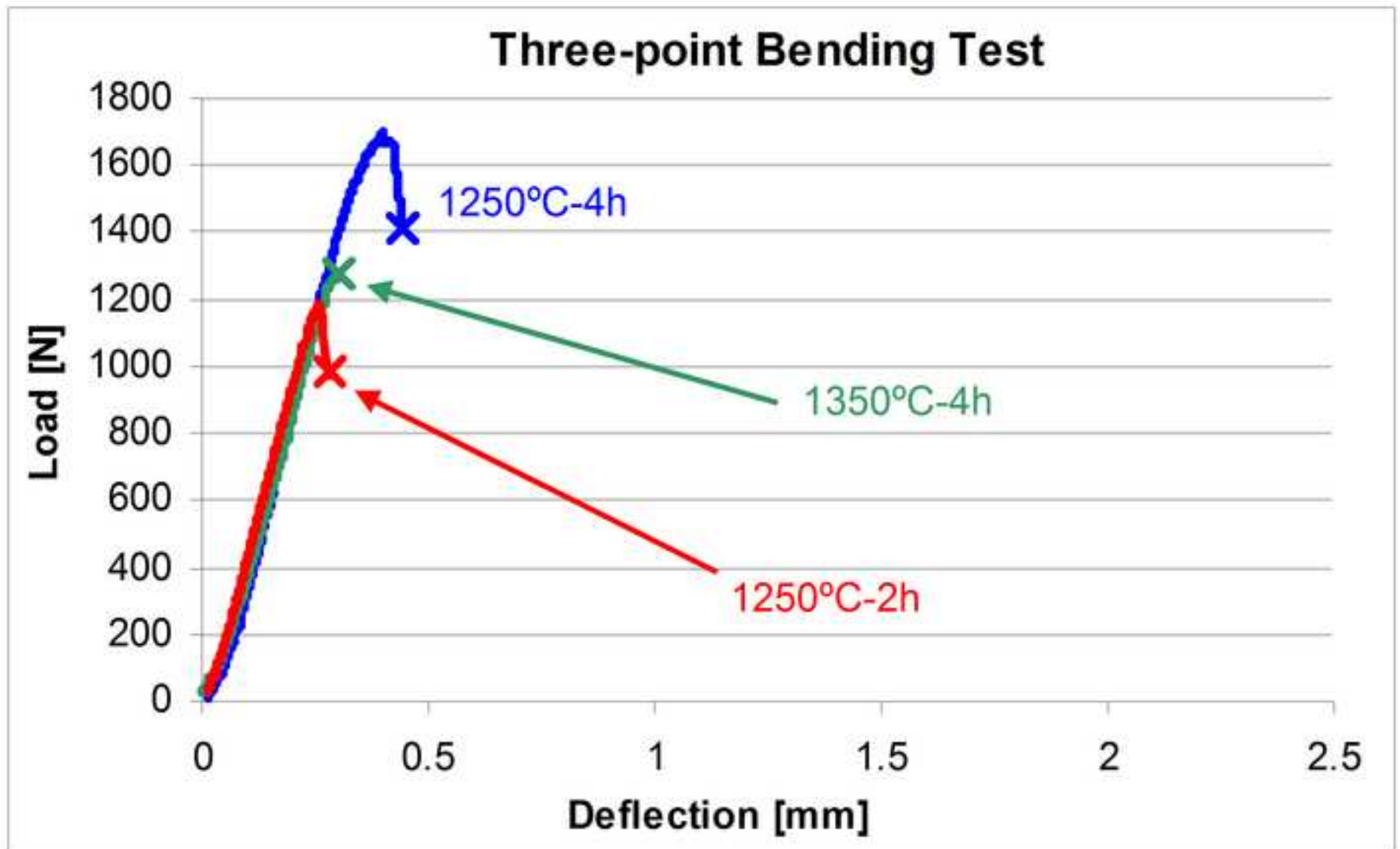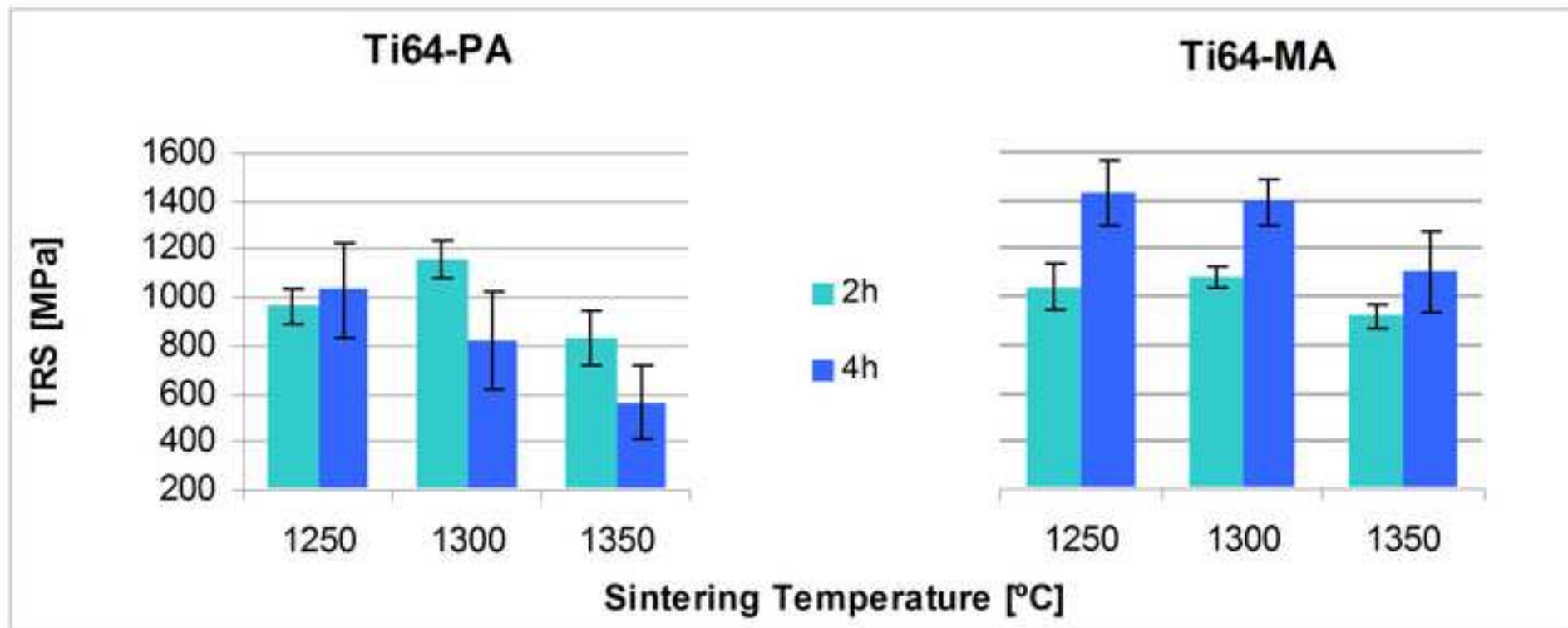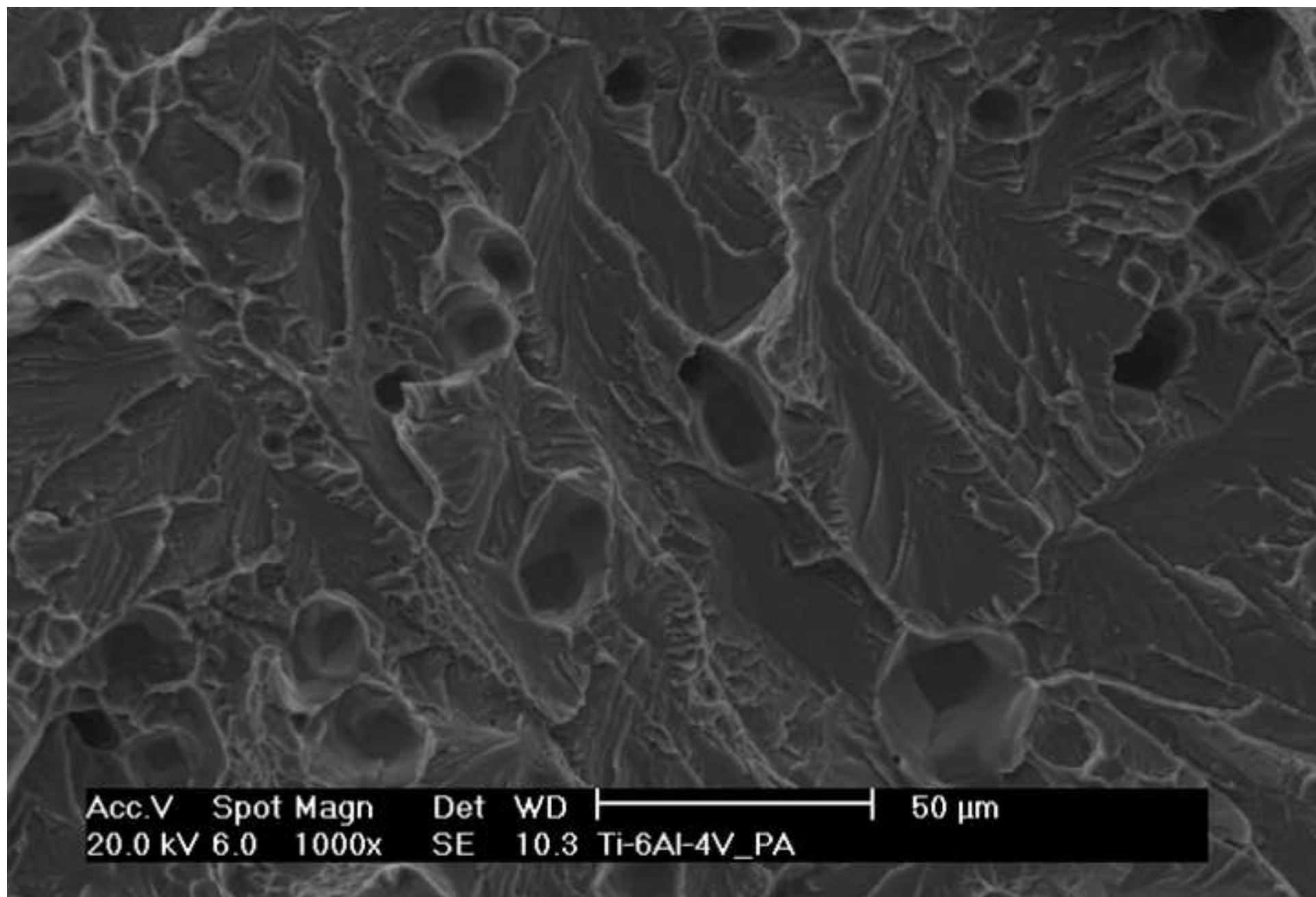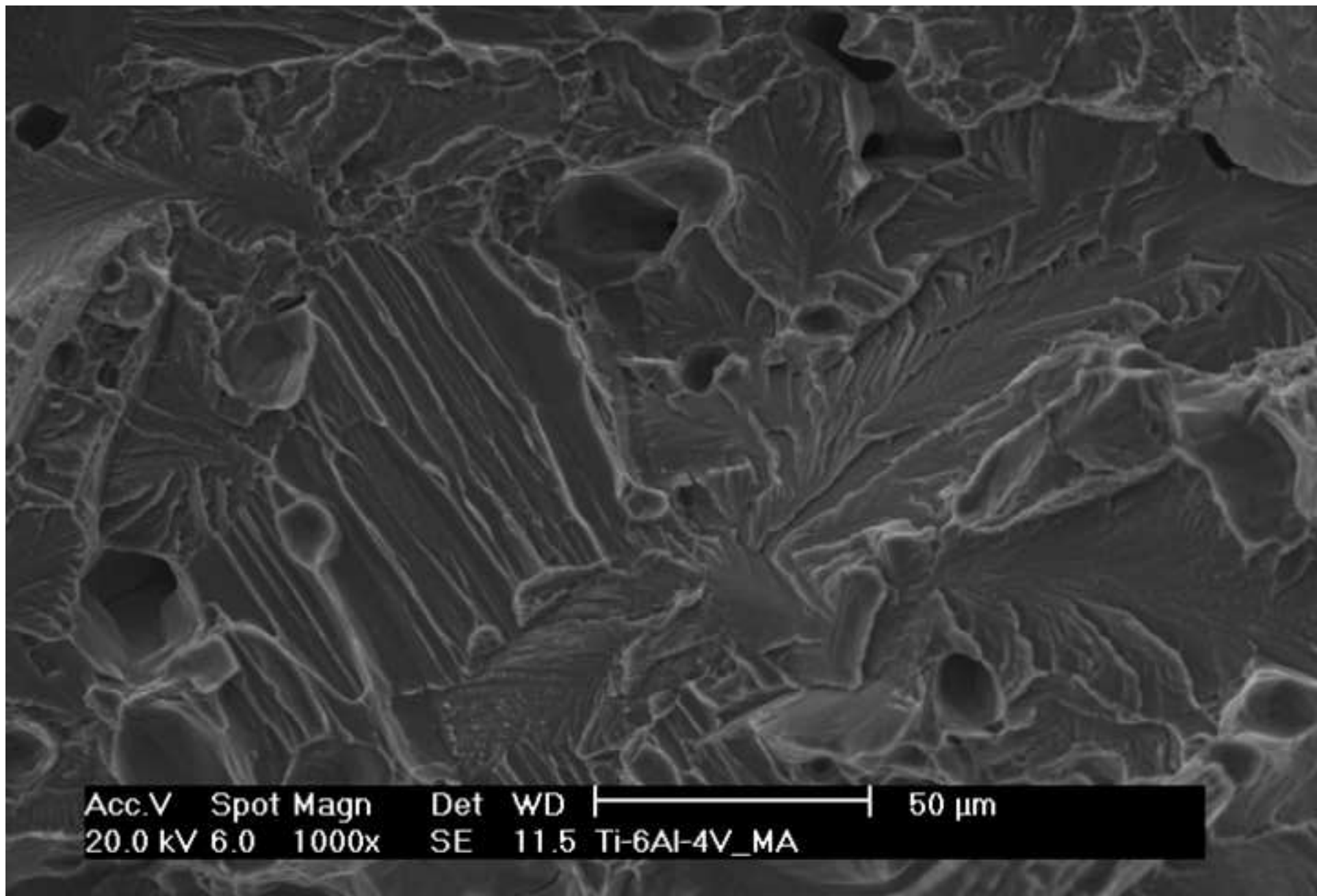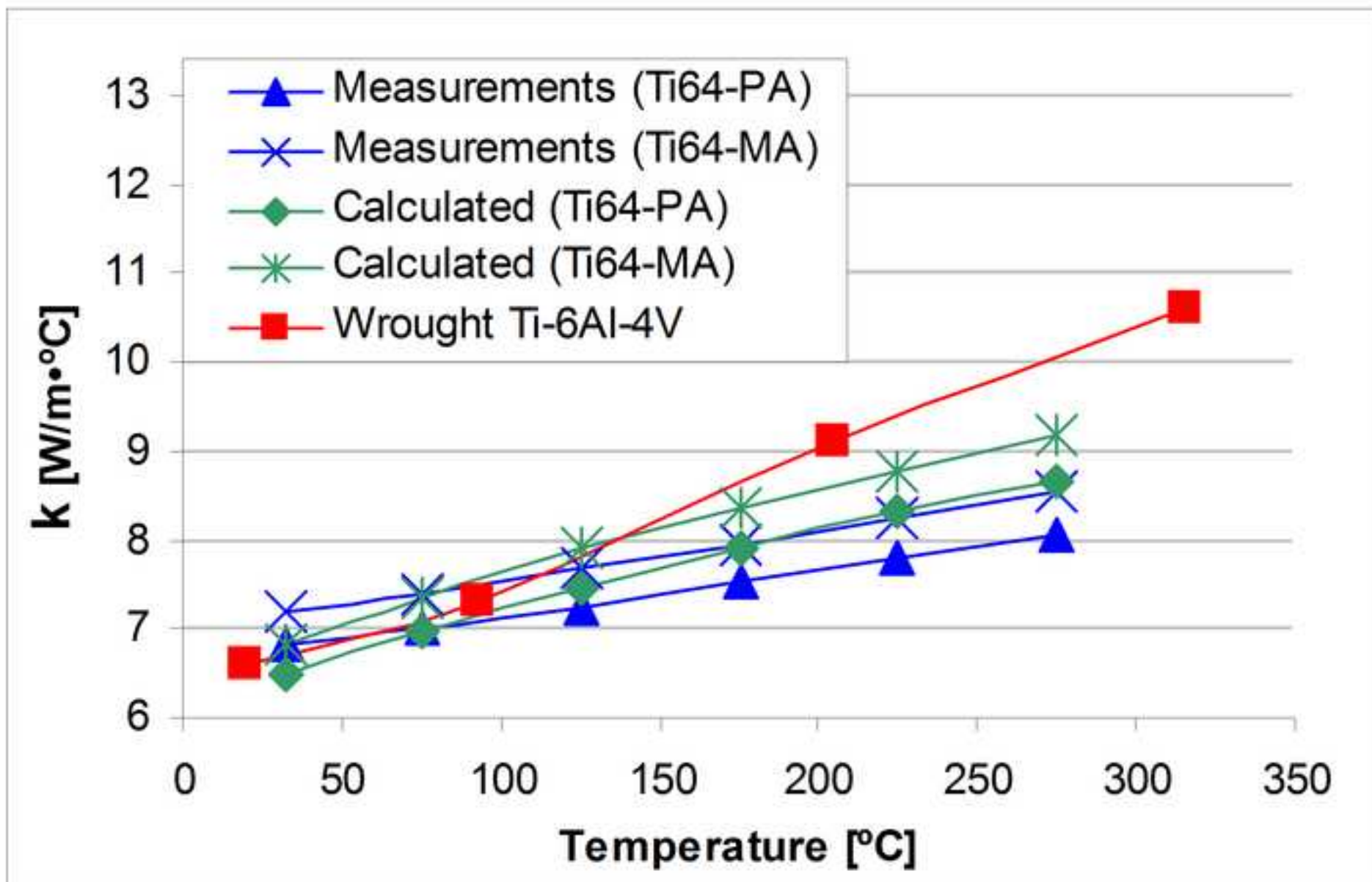
Table 1. Properties of the prealloyed and master alloys addition Ti-6Al-4V powders.

Alloy		*Ti-6Al-4V*	
Production method		Prealloyed (PA)	Master alloy addition (MA)
Morphology		Irregular	Irregular
Particle size distribution [%]	D_{10} [μm]	12.67	17.85
	D_{50} [μm]	31.78	42.94
	D_{90} [μm]	69.44	95.17

Table 2. Chemical analysis, thermal conductivity and electrical resistivity as a function of the processing parameters for prealloyed and master alloy addition Ti-6Al-4V sintered samples.

Material	Processing conditions	Chemical analysis		Property	
		Oxygen [wt.%]	*Nitrogen [wt.%]*	*Thermal Conductivity [W/m·K]*	*Electrical Resistivity [μΩ·cm]*
Ti64-PA	Starting powder	0.42 ± 0.01	0.007 ± 0.001	–	–
	1250ºC-2h	0.63 ± 0.04	0.023 ± 0.004	6.83	180.4
	1300ºC-2h	0.63 ± 0.06	0.027 ± 0.001	6.99	181.8
	1350ºC-2h	0.73 ± 0.15	0.022 ± 0.002	7.04	181.4
	1250ºC-4h	0.61 ± 0.14	0.019 ± 0.003	6.94	181.6
	1300ºC-4h	0.61 ± 0.07	0.020 ± 0.004	7.26	180.4
	1350ºC-4h	0.83 ± 0.12	0.019 ± 0.004	6.95	183.4
Ti64-MA	Starting powder	0.43 ± 0.07	0.012 ± 0.006	–	–
	1250ºC-2h	0.61 ± 0.01	0.022 ± 0.005	7.17	179.3
	1300ºC-2h	0.61 ± 0.01	0.018 ± 0.002	7.16	178.3
	1350ºC-2h	0.65 ± 0.03	0.020 ± 0.002	7.33	177.8

	1250ºC-4h	0.52 ± 0.02	0.022 ± 0.002	7.21	178.4
	1300ºC-4h	0.55 ± 0.03	0.026 ± 0.002	7.27	180.0
	1350ºC-4h	0.59 ± 0.03	0.022 ± 0.001	7.25	180.4
Ti-6Al-4V	Wrought	0.20 (max)	0.05 (max)	6.60	171.0

23

> The prealloyed and master alloy addition approaches to produce titanium alloys are compared. > The final properties are analyzed on the bases of the variation of the sintering temperature and time. > Flexural properties of PM Ti-6Al-4V are correlated with the influencing properties.> Determination of thermal conductivity and electrical resistivity of PM titanium based materials.